UC-404

LBL-27220
Preprint

Center for Advanced Materials

CAM

Submitted to Journal of Physical Chemistry

The Surface Structure and Chemical Reactivity of Rh(111)-(2×2)-3NO by HREELS and Dynamical LEED Analysis

C.-T. Kao, G.S. Blackman, M.A. Van Hove,
G.A. Somorjai, and C.-M. Chan

For Reference

Not to be taken from this room

August 1989

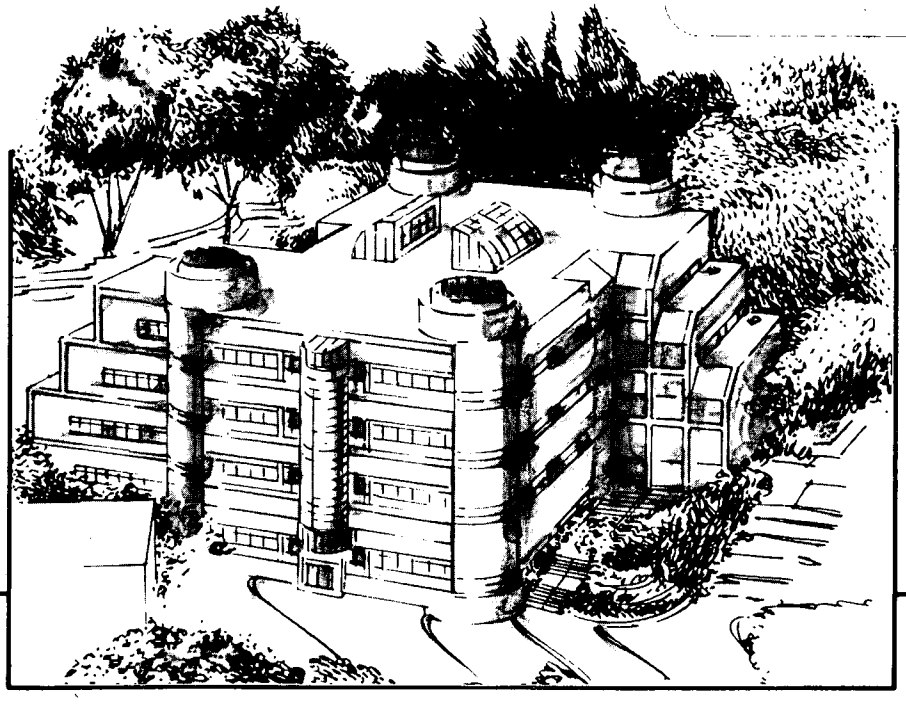

Materials and Chemical Sciences Division

Lawrence Berkeley Laboratory • University of California

ONE CYCLOTRON ROAD, BERKELEY, CA 94720 • (415) 486-4755

Prepared for the U.S. Department of Energy under Contract DE-AC03-76SF00098

LBL-27220
Copy 1
Bldg. 50 Library.

DISCLAIMER

This document was prepared as an account of work sponsored by the United States Government. While this document is believed to contain correct information, neither the United States Government nor any agency thereof, nor the Regents of the University of California, nor any of their employees, makes any warranty, express or implied, or assumes any legal responsibility for the accuracy, completeness, or usefulness of any information, apparatus, product, or process disclosed, or represents that its use would not infringe privately owned rights. Reference herein to any specific commercial product, process, or service by its trade name, trademark, manufacturer, or otherwise, does not necessarily constitute or imply its endorsement, recommendation, or favoring by the United States Government or any agency thereof, or the Regents of the University of California. The views and opinions of authors expressed herein do not necessarily state or reflect those of the United States Government or any agency thereof or the Regents of the University of California.

LBL-27220

The Surface Structure and Chemical Reactivity of Rh(111)-(2x2)-3NO by HREELS and Dynamical LEED Analysis

C.-T. Kao*, G.S. Blackman†, M.A. Van Hove and G.A. Somorjai
Center for Advanced Materials
Materials and Chemical Sciences Division
Lawrence Berkeley Laboratory
and
Department of Chemistry
University of California
Berkeley, CA 94720, USA
and
C.-M. Chan
Raychem Corporation
300 Constitution Drive
Menlo Park, CA 94025-1164, USA

August 5, 1989

*Present address:A.T.&T. Bell Laboratories, 600 Mountain Avenue, Murray Hill, NJ 07974, USA
†Present address: IBM Almaden Research Center, 650 Harry Road, San Jose, CA 95120-6099, USA

Abstract

The surface structure and chemical reactivity of nitric oxide on Rh(111) has been studied over the temperature range of 120-480 K by high-resolution electron energy loss spectroscopy (HREELS) and dynamical low-energy electron diffraction (LEED) analysis. HREELS results indicate that the adsorption sites of NO depend strongly on the surface coverage and adsorption temperature. At one-half monolayer coverage a c(4x2) LEED pattern is observed, with only bridge sites occupied (N-O stretching frequency of 1590 cm^{-1}). At saturation coverage and 120 K, only disordered bridge-site adsorption is observed (N-O stretching frequency of 1635 cm^{-1}). Saturation adsorption at a surface temperature between 250 K and 350 K leads to NO occupation of top sites (ν_{N-O}=1830 cm^{-1}) in addition to bridge sites (ν_{N-O}=1515 cm^{-1}), in an ordered (2x2) lattice. A dynamical LEED intensity analysis of the (2x2) structure shows that each unit cell contains two molecules in near-top-sites and one in a bridge site. All the NO molecules are perpendicular to the surface with bond lengths of 1.15Å. The Rh-N bond length is 2.07Å at the near-top site and 2.05Å at the bridge site. The NO surface structure is similar to a previously analyzed (2x2) structure at high CO coverage. This is the first LEED structural analysis for a pure molecular NO overlayer on a metal single crystal surface.

1 Introduction

The bonding and reactivity of nitric oxide on group VIII transition metal surfaces has been studied extensively. Group VIII metals such as rhodium, platinum, and palladium are active catalysts for the reduction of NO to N_2, which is an important process in automobile exhaust control [1]. Several recent studies have focused on kinetic studies of the NO reduction reaction with CO on platinum or rhodium foils and single crystals [2, 3]. Although there are several different suggested mechanisms for the NO reduction reaction on these surfaces, the dissociation of NO to form atomic oxygen and nitrogen is thought to be an important step of such reactions [4]. Fundamental chemisorption studies of nitric oxide on single-crystal surfaces should provide valuable insights into such a process.

Nitric oxide has a half-filled $2\pi^*$ antibonding orbital, which can either accept or donate electrons when it interacts with a metal surface [5, 6], whereas the empty $2\pi^*$ orbital of CO can only accept electrons. In metal-nitrosyl cluster compounds, the extra anti-bonding electron favors the formation of a bent NO specie for which there are no CO analogues [5, 7, 8]. The surface chemistry of NO is more complex than that of CO. The bond dissociation energy of NO (151 kcal/mole), is smaller than for CO (257 kcal/mole) on Rh(111) [9], and the dissociation process of NO to atomic oxygen and nitrogen was observed to be very sensitive to surface-defect concentration [10], coordination number [11], and surface coverage of NO [12].

Most of the surface structural information for NO chemisorption comes from studies with high-resolution electron energy loss spectroscopy (HREELS). A correlation between the observed N-O stretching frequencies and the possible bonding geometries has recently been summarized [13, 14]. Such a relationship is based on the comparison with the observed infrared (IR) frequencies in metal-nitrosyl cluster compounds, which have analogous local bonding geometries. A direct comparison of the NO surface structural determination with the bulk crystal structure of the metal-nitrosyl compound is necessary to justify such a surface-cluster bonding analogy.

The chemisorption of NO on Rh(111) has been studied by several research groups

by low-energy electron diffraction (LEED) [15], thermal desorption spectroscopy (TDS) [15, 16], x-ray photoelectron spectroscopy (XPS) [10], and HREELS [17]. The general observation is dissociative adsorption at low coverage and predominantly molecular adsorption at saturation dosage. At least two molecular states, β_1 and β_2, were observed for room-temperature adsorption by XPS [10]. Two ordered LEED patterns, c(4x2) and (2x2), were observed by Castner and Somorjai [15]. They suggested a structural model involving two different NO adsorption sites in a single (2x2) unit cell at 0.75-monolayer coverage (1 monolayer is defined as one molecule per surface metal atom).

The HREELS studies by Root et al. suggest a slightly different interpretation. They observe a single ν_{N-O} vibration in the HREEL spectra in the temperature range from 95-150 K, which they interpret as bridge-site NO at all coverages [17]. These authors also suggest that the (2x2) LEED pattern observed by Castner et al. is due to three domains of (2x1)-O from NO dissociation.

In order to resolve the disagreement between the studies at 95 and 300 K, we have performed our HREELS measurements at surface temperatures in the range of 120-480 K. At 120 K, a c(4x2) LEED pattern is observed around 0.8 L NO dosage, which corresponds to only bridge-site NO at half-monolayer coverage. A (2x2) pattern is produced by exposing the crystal to 5 L of NO at 250 K. The HREELS results indicate two new N-O stretch frequencies at 1515 and 1830 cm^{-1} for the (2x2) LEED pattern. This is in agreement with the LEED structural analysis for this (2x2)-3NO overlayer. Thus there is only one adsorption site at low temperatures (<120K) as found by Root et al.[17] and two adsorption sites at the higher temperatures (>250K) and higher coverages as suggested by Castner et al.[18] In this paper, we will discuss our HREELS data first, and then the LEED analysis. The structure of (2x2)-3CO on the same metal surface and the vibrational spectra of NO on other transition metal surfaces will also be compared.

2 Experimental

The experiments were carried out in two different stainless steel ultra-high vacuum chambers with base pressures of $2x10^{-10}$ torr. Each chamber is equipped with LEED, Auger Electron Spectroscopy (AES) and a mass spectrometer for TDS measurements as described in detail elsewhere [19, 20, 21, 22]. Briefly, one of the chambers has an HREEL spectrometer (we shall call it the "HREELS chamber"), which consists of 127° cylindrical monochromator and analyzer sectors with the total scattering angle fixed at 120°. For specular HREELS, the incidence and exit angles are $\theta_{in} = \theta_{out} = 60°$ from the surface normal, The overall system resolution (FWHM of the elastic peak) is 5 to 7.5 meV (40 to $60cm^{-1}$), and the incident beam current is $\sim 2x10^{-10}$ A at beam energies of 2 to 5 eV. All the HREEL spectra were recorded at either 95 K or room temperature after briefly annealing the adsorbed layer to the temperature indicated in the figures. All transformations with heating are irreversible.

The other chamber is designed for low-temperature LEED studies ("LEED chamber"). A single-stage closed-cycle helium refrigeration unit (Air Product, Displex OSP) was used to cool the sample down to about 40 K. Using electron bombardment heating, the sample could be heated to 1200 K in 60 seconds and cooled back down to 40 K in 90 seconds [22]. The (2x2) surface structure studied in the LEED chamber was prepared by exposing the crystal to 2.2 L of NO at 40K, followed by annealing to 220 K. The LEED data were collected at 40 K in order to reduce the thermal diffuse scattering. A video camera enclosed in a light-tight box was used to record the electron diffraction intensities over the energy range of 20-200 eV with 2 eV steps [23]. The images stored on video tape were later analyzed to produce the spot intensity versus voltage (I-V) curves [23, 24]. Altogether twenty-three groups of symmetrically equivalent I-V curves have been obtained at normal incidence(θ=0, ϕ=0). The orientation of the Rh(111) crystal was set by visual comparison of symmetrically equivalent spots. Two different Rh(111) single crystals were used during the course of the experiments; both were 0.5-1.0 cm^2 disks, 2 mm thick and cut from a single-crystal rod of $\geq$99.996% purity obtained from the Materials Research Cor-

poration. After polishing by standard methods [25, 26], the crystals were mounted in the two chambers, described previously [19, 22]. The single-crystal surfaces were cleaned by a combination of heating in oxygen, argon-ion sputtering and annealing in UHV until free of C, S, O, and B as detected by AES, LEED and HREELS [27].

The sample NO and O_2 gases (Matheson, 99%) were checked for purity by mass spectrometry and were used as received. Exposures are reported in Langmuirs [1 Langmuir(L)=10^{-6} torr-sec]. The dose pressure in the HREELS chamber has been corrected for five–fold enhancement of the molecular flux at the crystal surface due to a microcapillary array doser. In the low-temperature LEED chamber, the gases were adsorbed by backfilling the chamber. A multiplication factor of 3.5 is needed for comparison with the dosages in the HREELS chamber. The nitric oxide coverages were measured by using nitrogen and rhodium AES signals. They were calibrated by assuming a saturation coverage of 0.75 based on the observation of a sharp (2x2) LEED pattern at saturation dosage at 250-300 K. This is close to the reported 0.71 monolayer from previous XPS measurements at room temperature [10].

3 Results

3.1 Surface Ordering of NO in the Temperature Range 120-350 K

We have observed two ordered LEED patterns, c(4x2) and (2x2), at 0.5 and 0.75 monolayer coverages, respectively, in the temperature range 120-350 K. The c(4x2) pattern was produced by dosing 0.5-1.0 L NO at a surface temperature of 120 K. Subsequent annealing to temperatures above 320 K caused a disordering of the NO structure. The c(4x2) overlayer is extremely electron beam sensitive. An exposure of 100 μA-sec was sufficient to cause the fractional-order spots to disappear.

Two different methods were used to generate the NO (2x2) structures. In the LEED chamber a 2.2L dose of NO at 40K followed by annealing to 220K was sufficient to form the NO (2x2) pattern. In the HREELS chamber we dosed $\geq$ 5.0 L NO at a

surface temperature in the range 250-320 K. The (2x2) pattern disorders above 350 K regardless of exposure.

3.2 HREELS Studies of NO Chemisorption at 120-350 K

The HREEL spectra corresponding to the c(4x2) and (2x2) LEED patterns are shown in figures 1A and C, respectively. For figure 1A, 0.8 L of NO was adsorbed at 120 K. Two distinct vibrational modes, with frequencies at 435 and 1590 cm^{-1}, were observed. Increasing the dosage to 10.0 L at 120 K causes the 1590 cm^{-1} mode to shift up to 1635 cm^{-1}, as shown in figure 1B. The low-frequency mode near 435 cm^{-1} shifts down slightly to 405 cm^{-1}.

Other surface species, such as $(NO)_2$ dimers [28], NO_2 [29], or N_2O [30], can be ruled out due to the simplicity and position of the observable modes. The presence of multilayer NO is unlikely at this temperature (the desorption temperature of multilayer NO adsorbed on metal surfaces is around 100 K [31]). We see no vibrational mode around 1876 cm^{-1}, which is the characteristic N-O stretch mode of physisorbed nitric oxide measured by infrared spectroscopy [32]. We therefore assign the peaks at 435 and 1590 cm^{-1} in figure 1A to Rh-NO and N-O stretching frequencies, respectively. The observed shifts of the N-O stretching modes in both figures 1A and 1B, relative to gas-phase NO, are in the range of 240-280 cm^{-1}. This is indicative of new chemisorbed molecular NO states on Rh(111) at 120 K.

The number of observed dipole-active modes in the specular HREEL spectra can be used to determine the symmetry of the NO bonding geometry. On an fcc(111) surface there are four most probable NO bonding geometries. For NO adsorption at top, bridge, or hollow sites with the N-O axis perpendicular to the surface plane, the dipole active modes are the ν(metal-NO) and ν(N-O) stretching frequencies [13]. For a bent bonding geometry the surface symmetry is C_s, and the expected dipole active vibrational modes are ν(N-O), ν(metal-NO), and two δ(metal-NO) bending modes. One of the δ(metal-NO) modes, a frustrated translational mode, is usually below the scanning range of the HREEL spectrum ($\leq$200 cm^{-1}) [13, 14], but we still expect three dipole-active modes for a bent geometry. There are only two features

for NO in figures 1A and 1B; therefore, we believe that the surface symmetry of NO is higher than C_s and that the most likely structure for NO on Rh(111) has the N-O axis normal to the surface.

We now compare the observed N-O stretching modes on a Rh(111) surface to those of analogous metal-nitrosyl cluster compounds. Based on infrared and x-ray crystallographic analyses of metal-nitrosyl complexes, it is usually suggested that N-O vibrational frequencies in the range 1650-2000 cm^{-1} correspond to linearly bonded NO [5], those in the range 1480-1550 cm^{-1} correspond to twofold bridge coordination [33], while those in the range 1320-1410 cm^{-1} correspond to threefold hollow coordination [34, 35]. The bent NO configuration would have two modes, a ν(N-O) stretching mode in the range 1530-1700 cm^{-1} and a δ(N-O) bending mode around 700 cm^{-1} [7, 8, 14]. Although our observed N-O stretch, 1590-1635 cm^{-1}, is within the range of terminal bent metal-nitrosyl compounds, the number of observable modes in the specular direction is more consistent with a high-symmetry bonding site. This implies that either the top or the bridge site is a more probable adsorption site for NO on Rh(111).

If we dose an additional 25 L of NO at a surface temperature of 250 K after the 10 L dosage at 120 K, a (2x2) LEED pattern is observed. Three new vibrational peaks, at 485, 1515, and 1830 cm^{-1}, are observed in the HREEL spectrum, as shown in figure 1C. A similar spectrum is observed at saturation coverage for surface temperatures in the range 250-320 K. The only difference is that the 1630 cm^{-1} mode intensity decreases as the NO is adsorbed at higher temperatures. If we adsorb NO at a surface temperature of 300 K or above, the high frequency peak almost disappears. At 350 K both vibrational modes disappear, as does the LEED pattern.

Based on the HREELS data, we believe that there are two major NO species coexisting in the (2x2) ordered overlayer. Both the 1830 cm^{-1} and 1515 cm^{-1} peaks are in the range of N-O stretching frequencies for terminal and bridge-bonded metal-nitrosyl complexes. We assign these to top and twofold bridge-site NO, respectively. The two peaks at 400 and 485 cm^{-1} can be attributed to Rh-NO stretching frequencies for these two species.

In figure 1C, the intensity ratio of the N-O stretching frequencies for NO at top (1840 cm^{-1}) and bridge sites (1515 cm^{-1}) is about 2:1. This is similar to the HREEL spectrum of the (2x2)-3CO structure, where two near-top sites and one bridge site were also found to exist in each unit cell [36, 37].

3.3 HREELS Studies of Chemisorbed NO at 350-480 K

After annealing the saturated surface to 360 K, the (2x2) LEED pattern disappears and the HREEL spectrum shows significant changes (see figure 2B). The top-site NO with characteristic ν(N-O) and ν(Rh-NO) vibrational modes at 1830 and 480 cm^{-1} disappears by 360 K, which is the temperature at which NO starts to desorb [15, 16]. The features in figure 2B are similar to those in figure 1B, and thus only bridge-bonded molecular NO species exist on the surface. No mode is observed at 520-580 cm^{-1}, where the Rh-O stretch could appear for atomic oxygen from NO dissociation.

At surface temperatures above 360 K, the 1630 and 405 cm^{-1} modes gradually disappear. By about 480 K a new vibrational peak appears at 530 cm^{-1}, as shown in figure 2C. From previous TDS studies [15, 16], the desorption of NO at 350-450 K is known to be accompanied by dissociation to atomic nitrogen and oxygen. The resulting nitrogen desorbs in the temperature range 400-700 K, followed by oxygen desorption at 1000-1400 K. At 480 K all molecular species are either dissociated or desorbed, and most of the atomic nitrogen is expected to have recombined to desorb as molecular nitrogen. The major surface species left is atomic oxygen. We therefore assign the 530 cm^{-1} peak to the Rh-O stretching frequency of atomic oxygen from NO dissociation. The two small peaks, at 1490 and 2030 cm^{-1}, can be assigned to ν(N-O) and ν(C-O) from background adsorption during our data collection.

4 LEED Intensity Analysis

4.1 LEED Theory

We have applied LEED calculational methods that are very similar to those used in the structural analysis of the Rh(111)-(2x2)-3CO structure [36, 37]. Those methods

explored the validity of a number of approximations so that we can apply them now with confidence. For the NO adsorption structure, we have chosen to ignore the multiple scattering occurring between molecules. This leads to what we now call "kinematic sublayer addition" (KSLA) within the "beam set neglect" (BSN) method [21, 38]. All multiple scattering is allowed within individual molecules, by means of "matrix inversion" in the spherical-wave representation [39, 40]. With this approximation and for the relatively close-packed molecular layers in question, the structural uncertainties are maintained within 0.1 $\AA$ [36, 37]. Between the substrate layers and between the overlayer and the substrate, we use renormalized forward scattering in the plane-wave representation.

The physical parameters used in the calculations are the same as those in the earlier CO calculations [36, 37]. The only exceptions are different phase shifts for NO, obtained from a cluster calculation of NO on 8 Rh atoms. Theory and experiment were, as usual in our molecular overlayer studies, compared with a set of five R-factors and their weighted average value [36, 37]. These include both the Zanazzi-Jona and Pendry R-factors.

4.2 Structural Determination

Based on our earlier analysis of the analogous (2x2)-3CO overlayer [36, 37] and based on the evidence from HREELS, we have made the following structural assumptions for Rh(111)-(2x2)-3NO. The substrate is taken to be bulk-like. The NO molecules are taken to be intact and perpendicular to the surface. Three NO molecules fit in each (2x2) unit cell (but we have also investigated one molecule per cell). The molecules tend toward high-symmetry sites like top, bridge, and hollow sites, to the extent compatible with close packing. In each structure tested the N-O bond length was kept the same for all molecules, but that common length was allowed to vary.

The best-fit model is shown in figure 3. In this model, one of the three NO molecules in the unit cell occupies a bridge site, while the two other NO molecules occupy equivalent "near-top" sites: we label this model "1-bridge/2-top." Here the symmetrical bridge site fixes the structure, while the NO molecules in the near-top

sites adjust themselves accordingly.

We also tried a "1-top/2-bridge" model, in which the role of the bridge and top sites is reversed. It is obtained from the "1-bridge/2-top" model of figure 3 by a shift of the overlayer such that the bridge-site NO molecules end up exactly and symmetrically at the top sites. The two other NO molecules then adjust themselves at near-bridge sites.

For comparison, we have also tested several structures with just one NO molecule per unit cell. The four high-symmetry sites were explored: top, bridge, hcp-hollow and fcc-hollow.

In all cases, we have varied the Rh-N interlayer spacings [$d_{\perp}$(Rh-NO)], as well as the N-O bond-length [$d_{\perp}$(N-O)], as table 1 summarizes. For the structure models of "1-top/2-bridge" and "1-bridge/2-top", the parallel [$d_{\parallel}$(N-N)] and perpendicular [$d_{\perp}$(N-N)] distances for two types of NO within the (2x2) lattice were also adjusted, as listed in table 1.

Table 2 shows, for each basic model, the best-fit structural parameters and the R-factor value achieved. The models with only one NO per (2x2) cell have much higher R–factors. The 1-bridge/2-top model is favored, while the 1-top/2-bridge model gives a theory-experiment fit of comparable quality. It has somewhat different bond lengths than for the 1-bridge/2-top model, and they are less realistic: we therefore consider this model unlikely. The best structure is tabulated in the SCIS format [41] in table 3.

Our best 5-R-factor-average value of 0.279 can be compared with the value of 0.19 for the analogous CO structure (which used a better theoretical approximation, thereby in part improving the R-factor) [36, 37]. The simpler Rh(111)-($\sqrt{3}$ x$\sqrt{3}$)R30°-CO structure yielded an R-factor value of 0.23 [42]. The coadsorption structures of NO or CO with ethylidyne (CCH_3) gave best-fit R-factor values of 0.294 and 0.242, respectively. [22]

5 Discussion

5.1 Surface Ordering of NO on Rh(111)

A (2x2) LEED pattern was observed at saturation coverage of nitric oxide on Rh(111) at temperatures in the range 250-350 K. This is in agreement with previous work by Castner and Somorjai [15]. However, Root et al. reported a streaky (2x2) pattern at 250 K after adsorbing NO at 95 K, which they attributed to three (2x1) domains of atomic oxygen from NO decomposition upon annealing [17]. We can rule out this interpretation of the (2x2) pattern by comparing the I-V curves for the three different structures. In figure 4 are compared LEED I-V curves for the (1, -1/2) beam of the (2x2)-3NO structure, the (2x1)-O structure [39] and the (2x2)-3CO structure [36, 37]. Important differences can be seen between the curves for (2x2)-3NO and for (2x1)-O, while many similarities in peak positions exist between the curves for (2x2)-3NO and for (2x2)-3CO.

It is unlikely that domains of 0.5-monolayer oxygen from NO dissociation exist at 250 K. Only 3% of saturation NO coverage was reported to dissociate at room temperature, based on previous XPS measurements [10]. The difference between our (2x2) pattern and the patterns observed previously [17] could be due to differences in adsorption temperature and dosing pressure [37], defect concentration [10], or small amounts of surface contaminant present on the Rh(111) crystal surface [43]. All of these factors could change the surface oxygen and nitrogen atom concentrations from NO decomposition at $T \geq 250$ K, and this could lead to changes in the surface coverage, adsorption site, and fragmentation probability for the NO molecule.

At 120-320 K, a c(4x2) LEED pattern was observed for half a monolayer of NO adsorbed on Rh(111). The observed N-O stretch at 1590 cm^{-1} shown in figure 1A is consistent with a previously published frequency [17] and with bridge-site adsorption. A similar pattern and coverage for NO adsorption on a Pd(111) surface were reported by Conrad et al. [44].

5.2 Surface Structure of Rh(111)-(2x2)-3NO

Root et al. previously studied NO adsorption at 95 K on Rh(111) by HREELS

[17]. A gradual shift in the ν(N-O) stretch from 1480 to 1630 cm^{-1} from 0.025 to 0.68 monolayer coverage was reported in their work. They attribute the shift of the N-O stretching mode to a coverage-dependent dipole-dipole interaction of bridge-site NO. Our data at 120 K are within the range of the medium (0.5) to high coverage (0.68) of NO reported by Root et al. [17] The N-O stretch frequency of the c(4x2)-NO structure shown in figure 1A is 1590 cm^{-1}, in accordance with previous results at 0.50-monolayer coverage. The N-O stretch for the 10 L NO dosage at 1635 cm^{-1} is close to the 0.68 monolayer of NO reported at 95 K. The ν(Rh-NO) modes at 405 and 435 cm^{-1} in figure 1A and 1B are better resolved in this work, while a broad loss peak near 360 cm^{-1} with high background intensity was observed previously [17]. Our HREELS results in the low coverage regime are in accord with previous results.

Figure 3 shows top and side views of the best-fit structure for (2x2)-3NO by dynamical LEED analysis. One of the NO molecules is located on a pure bridge site, while the other two are pushed slightly off the top sites. The two near-top-site NO molecules have their molecular axis shifted by 0.26 $\AA$ from the center of the metallic rhodium atom. A similar distortion was noted for the Rh(111)-(2x2)-3CO structure, but the molecular axis was shifted an additional 0.26 $\AA$ compared to the NO overlayer, i.e. by a total of 0.52 $\AA$ [36, 37]. The difference can be ascribed to the smaller Van der Waals size of the nitrogen atom compared to the carbon atom, as illustrated in figure 5. The tighter packing of CO compared to NO is likely to be responsible for the more difficult preparation of the CO overlayer: the CO overlayer forms only with a background pressure above 10^{-6} torr, while for NO an exposure of 25 L at 10^{-7} torr is sufficient to generate a (2x2) LEED pattern at 250K.

In table 4, we summarize the structural parameters of both (2x2)-3NO and (2x2)-3CO, as well as the previously analyzed LEED structures of ($\sqrt{3}$ x $\sqrt{3}$)R30°-CO, c(4x2)-CCH_3+NO and c(4x2)-CCH_3+CO, all on Rh(111). In this table, adsorption site, bond length and interlayer spacing are all listed for direct comparison. These results agree reasonably well (within the error bars indicated) among themselves. However, the Rh-NO bond length for the top site seems somewhat large compared to the analogous Rh-CO bond length, even after taking the slightly larger N covalent

radius into account.

The present surface structure determination is also in agreement with the bond lengths of analogous metal-nitrosyl compounds, as determined by x-ray crystallography [45, 46]. For example the two-fold coordinated NO ligands in $Ru_3(CO)_{10}(NO)_2$ [47] each have Ru-NO bond lengths of 2.03Å.

The (2x2)-3NO structure is the first complete structural analysis for a pure molecular NO overlayer on transition metal surfaces and is also the first direct calibration for an HREELS assignment of NO adsorption sites by LEED crystallography.

5.3 Surface Chemical Bond of NO Adsorbed on Transition Metal Surfaces

We now compare our results with NO adsorption on other transition metal surfaces. Most structural information has relied on the application of vibrational spectroscopy: both HREELS and reflection-absorption infrared spectroscopy (RAIRS) have been used. The observed vibrational frequencies for NO adsorbed on various metal surfaces are summarized in table 5. Sequential adsorption at different bonding sites is generally observed. For instance, on Ru(001) at a surface temperature of 120 K, NO adsorbs first at the threefold hollow site at low coverage followed by the twofold bridge and top sites at higher coverages [48, 49, 50]. For our study on Rh(111), and for the work on Pd(111) [51], Pt(111) [52, 53, 54], and Pd(100) [55], bridge-site NO is followed by top-site NO at near-saturation coverage.

Another type of bonding geometry has been proposed on several metal surfaces: bent NO with a metal-N-O bond angle in the approximate range 120-140°. The substrates include Pt(100)-(1x1) [14], Pt(100)-(5x20) [14, 56], Ni(111) [12], and Rh(100) [57]. The reported δ(M-NO) and ν(N-O) frequencies extend from 380 to 840 cm^{-1} and 910 to 1790 cm^{-1}, respectively, as shown in table 3. Surface crystallographic studies are necessary to confirm this bent NO bonding geometry.

The adsorption sites of NO are dependent on surface temperature. On Ru(001), a metastable top-site NO was observed at 78 K. Subsequent annealing to 120 K caused an irreversible top-to-bridge-site transformation [31]. The barrier to such surface hop-

ping was determined to be 5.9 kcal/mole. On Rh(111), as shown in figure 1A and 1B, bridge-site NO is the predominant species at temperatures between 95 and 120 K [17], while saturation adsorption at 250 K produces some top-site species in the compact (2x2)-3NO overlayer. Previous studies have indicated significant surface diffusion of NO on Rh(111) at 250 K [2]. The barrier to surface diffusion has been recently measured to be 7.0 kcal/mole by the laser-induced surface diffusion technique [58]. We believe this could be one of the reasons why the compression of (2x2)-3NO was observed only by heating to 250 K on Rh(111).

The adsorption behavior of NO on the Pd(111) surface studied appears to be similar to that on Rh(111). Recent HREELS studies indicate that the adsorption site of NO on Pd(111) depends on surface temperature and coverage [51]. The observed N-O and Pd-NO stretching frequencies on Pd(111) are included in table 3. Bridge-site NO, with an N-O stretch in the range 1510-1660 cm^{-1}, populates first at both 130 K and room temperature; but top-site NO, with ν(N-O) in the range 1720-1830 cm^{-1}, exists only below 250 K at high surface coverage on Pd(111). At room temperature all the top-site NO desorbs first, followed by bridge-site desorption at 400 K. Two ordered structures, c(4x2) and (2x2), at 0.5 and 0.75 monolayer coverages, respectively, were also found for NO adsorption on Pd(111) at 130 K [44, 51]. Similar structural models can be proposed for the c(4x2) and (2x2) NO overlayers on Pd(111).

The similarity of NO chemisorption on Rh(111) and Pd(111) at low temperature is in contrast to the case of CO adsorption: top-site CO populates first on Rh(111) [42], while the threefold hollow-site CO is the favored species on Pd(111) at low coverages [59, 60].

5.4 Reactivity of Nitric Oxide on Metal Surfaces

Based on the observed spectra shown in figure 2, we believe that the top-site NO on Rh(111) either desorbs or shifts to bridge-site NO instead of dissociating; however, the bridge-site NO is the major contributor to the dissociation of NO to atomic oxygen and nitrogen in the temperature range 350-480 K. Similar findings have been reported on other metal surfaces, such as Ru(001) [50]. The desorption

and dissociation barriers of bridge-site NO on Rh(111) were previously measured to be 30 kcal/mole and 19.2 kcal/mole, respectively [16, 17].

On the Rh(100) surface, where a bent NO bonding geometry was proposed based on HREELS [57], the observed dissociation barrier is 10.5 kcal/mole, with dissociation starting at 170 K. Rh(100) is more reactive toward NO dissociation than the hexagonal close-packed Rh(111) surface. Recent XPS and field electron microscopy studies have reported an even higher reactivity on Rh(331) and Rh(321) surfaces, where lower-coordination sites at step and kink positions have high surface concentrations [61]. This trend of surface reactivity has been modeled with reasonable success by Banholzer et al [62] using rules of conservation of orbital symmetry. The proposed active site for NO dissociation consists of a specific arrangement of atoms instead of just a single step on the surface [63].

Not only does the reactivity toward NO dissociation depend strongly on crystallographic orientation, but it also depends on the substrate material. Dissociative chemisorption is generally observed for NO adsorption at room temperature on the transition metals to the left in the Periodic Table. This includes the W(100) [64], Fe(110) [65], and Re(0001) [66] surfaces; however, on the metals to the right in the Periodic Table, such as Pd(111) [44, 51] and Pt(111) [52, 53, 54], associative adsorption is the predominant process at room temperature.

6 Conclusions

The major points of this paper are as follows:

- Two ordered molecular NO structures, c(4x2) and (2x2), are observed at NO coverages of 0.5 and 0.75 monolayers, respectively, in the temperature range 120-350 K. Based on the HREELS data and the LEED pattern, the c(4x2) unit cell contains two equivalent bridge-site NO molecules with ν(N-O) and ν(Rh-NO) frequencies of 1630 and 405 cm^{-1}, respectively.

- The first complete LEED analysis has been performed for the (2x2)-3NO structure. The best structural model, with an 0.279 R-factor, consists of two near-top

and one bridge-site NO molecules in each unit cell. This is similar to the model determined for (2x2)-3CO on the same metal surface. A 0.26 Å lateral shift from the symmetrical top site is observed for (2x2)-3NO and is attributed to tight packing of adsorbates that prevents top-site occupation.

- The surface ordering and structure of NO on Rh(111) is similar to that on Pd(111). Rh(111) is observed to be more reactive to NO dissociation at 360-480 K than is Pd(111), but it is less reactive than the Rh(100) surface. The dissociation of nitric oxide on these transition metals is, therefore, a structure-sensitive reaction.

Acknowledgements

This work was supported in part by the Director, Office of Energy Research, Office of Basic Energy Sciences, Materials Sciences Division of the U.S. Department of Energy under Contract No. DE-AC03-76SF00098. C.-T. Kao gratefully acknowledges a predoctoral fellowship from B.P.-America Corp.

References

[1] W.F. Egelhoff, Jr. *Chemical Physics of Solid Surfaces and Heterogeneous Catalysis*, chapter 9. Volume 4, Elsevier, Amsterdam, 1982.

[2] T.W. Root, L.D. Schmidt, and G.B. Fisher. *Surf. Sci.* **150** (1985) 173.

[3] G.A. Papapolymerou and L.D. Schmidt. *Langmuir* **1** (1985) 488.

[4] R.E. Hendershot and R.S. Hansen. *J. Catalysis* **98** (1986) 150.

[5] F.A. Cotton and G. Wilkinson. *Advanced Inorganic Chemistry.* Wiley, New York, 3 edition, 1972.

[6] S.-S. Sung, R. Hoffmann, and P.A. Thiel. *J. Phys. Chem.* **90** (1986) 1380.

[7] C.C. Su and J.W. Faller. *J. Organomet. Chem.* **84** (1975) 53.

[8] JANAF. *Thermochemical Tables.* Volume 37 of *Natl. Stand. Ref. Data Ser.*, Natl. Bur. Stand., 2 edition, 1971.

[9] J.B. Benziger. *Appl. Surf. Sci.* **6** (1980) 105.

[10] L. A. DeLouise and N. Winograd. *Surf. Sci.* **159** (1985) 199.

[11] R.I. Masel. *Catal. Rev.-Sci. Eng.* **28** (1986) 335.

[12] S. Lehwald, J.T. Yates, Jr., and H. Ibach. *Proceedings of the Fourth International Conference on Solid Surfaces*, page 221. Institute of Physics and Physical Society, London, 1980.

[13] H. Ibach and D.L. Mills. *Electron Energy Loss Spectroscopy and Surface Vibrations.* Academic, New York, 1982.

[14] G. Pirug, H.P. Bonzel, H. Hopster, and H. Ibach. *J. Chem. Phys.* **71** (1979) 593.

[15] D.J. Castner, B.A. Sexton, and G.A. Somorjai. *Surf. Sci.* **71** (1978) 519.

[16] T.W. Root, L.D. Schmidt, and G.B. Fisher. *Surf. Sci.* **134** (1983) 30.

[17] T.W. Root, G.B. Fisher, and L.D. Schmidt. *J. Chem. Phys.* **85** (1986) 4679.

[18] D.G. Castner, B.A. Sexton, and G.A. Somorjai. *Surf. Sci.* **71** (1978) 519.

[19] B.E. Koel, J.E. Crowell, C.M. Mate, and G.A. Somorjai. *J. Phys. Chem.* **88** (1984) 1988.

[20] A.L. Cabrera, N.D. Spencer, E. Kozak, P.W. Davis, and G.A. Somorjai. *Rev. Sci. Instr.* **53** (1982) 1888.

[21] R.F. Lin, G.S. Blackman, M.A. Van Hove, and G.A. Somorjai. *Acta Crystallogr. B* **43** (1987) 368.

[22] G.S. Blackman, C.-T. Kao, B.E. Bent, C.M. Mate, M.A. Van Hove, and G.A. Somorjai. *Surf.Sci.,* (1989) in press.

[23] D.F. Ogletree. PhD thesis, University of California, Berkeley, 1986.

[24] D.F. Ogletree, G.A. Somorjai, and J.E. Katz. *Rev. Sci. Inst.* **57** (1986) 3012.

[25] R.J. Koestner, M.A. Van Hove, and G.A. Somorjai. *Surf. Sci.* **121** (1982) 321.

[26] R.C. Yeates. PhD thesis, University of California, Berkeley, 1985.

[27] S. Semancik, G.L. Haller, and J.T. Yates, Jr. *Appl. Surf. Sci.* **10** (1982) 133.

[28] C.E. Dinerman and G.E. Ewing. *J. Chem. Phys.* **53** (1970) 626.

[29] M.E. Bartram, R.G. Windham, and B.E. Koel. *Surf. Sci.* **184** (1987) 57.

[30] N.R. Avery. *Surf. Sci.* **131** (1983) 501.

[31] U. Schwalke and W.H. Weinberg. *J. Vac. Sci. Technol. A* **5** (1987) 459.

[32] K. Nakamoto. *Infrared and Raman Spectra of Inorganic and Coordination Compounds.* Wiley, New York, 1977.

[33] R.B. King and M.B. Bisnette. *J. Am. Chem. Soc.* **85** (1963) 2527.

[34] R.C. Elder, F.A. Cotton, and R.A. Schunn. *J. Am. Chem. Soc.* **89** (1967) 3645.

[35] J. Muller and S. Schmidt. *J. Organometa. Chem.* **97** (1975) C54.

[36] M.A. Van Hove, R.J. Koestner, and G.A. Somorjai. *Phys. Rev. Lett.* **50** (1983) 903.

[37] M.A. Van Hove, R.J. Koestner, J.C. Frost, and G.A. Somorjai. *Surf. Sci.* **129** (1983) 482.

[38] M.A. Van Hove, R.F. Lin, and G.A. Somorjai. *Phys. Rev. Lett.* **51** (1983) 778.

[39] M.A. Van Hove, W.H. Weinberg, and C.M. Chan. *Low Energy Electron Diffraction.* Springer Verlag, Heidelberg, Berlin, New York, 1986.

[40] M.A. Van Hove and S.Y. Tong. *Surface Crystallography by LEED.* Springer Verlag, Heidelberg, Berlin, New York, 1979.

[41] J.M. MacLaren, J.B. Pendry, P.J. Rous, D.K. Saldin, G.A. Somorjai, M.A. Van Hove, and D.D. Vvedensky. *Surface Crystallographic Information Service: A Handbook of Surface Structures.* D. Reidel Publishing Company (Dordrecht, Holland), 1987.

[42] R.J. Koestner, M.A. Van Hove, and G.A. Somorjai. *Surf. Sci.* **107** (1981) 439.

[43] F. Solymosi and J. Sarkany. *Appl. Surf. Sci.* **3** (1979) 68.

[44] H. Conrad, G. Ertl, J. Küppers, and E.E. Latta. *Surf. Sci.* **65** (1977) 235.

[45] M.R. Albert and J.T. Yates, Jr. *The Surface Scientists Guide to Organometallic Chemistry.* ACS, Washington, D.C., Washington, D.C., 1987.

[46] J.P. Collman and L.S. Hegedus. *Principles and Applications of Organotransition Metal Chemistry.* University Science Books, Mill Valley, 1980.

[47] Jack R. Norton, James P. Collman, Guiliano Dolcetti, and Ward T. Robinson. *Inorganic Chemistry* **11(2)** (1972) 382.

[48] P.A. Thiel, W.H. Weinberg, and J.T. Yates, Jr. *Chem. Phys. Lett.* **67** (1979) 403.

[49] P.A. Thiel, W.H. Weinberg, and J.T. Yates, Jr. *J. Chem. Phys.* **71** (1979) 1643.

[50] H. Conrad, R. Scala, W. Stenzel, and R. Unwin. *Surf. Sci.* **1** (1984) 145.

[51] I. Harrison, C.-T. Kao, and G.A. Somorjai. 1989. to be published.

[52] H. Ibach and S. Lehwald. *Surf. Sci.* **76** (1978) 1.

[53] B.A. Gland, J.B. Sexton. *Surf. Sci.* **94** (1980) 355.

[54] B.E. Hayden. *Surf. Sci* **131** (1983) 419.

[55] S.W. Jorgensen, N.D.S. Channing, and R.J. Madix. *Surf. Sci.* **179** (1987) 322.

[56] W.F. Banholzer and R.I. Masel. *Surf. Sci.* **137** (1984) 339.

[57] J.S. Villarrubia and W. Ho. *J. Chem. Phys.* **87** (1987) 750.

[58] E.G. Seebauer, A.C.F. Kong, and L.D. Schmidt. *J. Vac. Sci. Technol. A* **5** (1987) 464.

[59] A.M. Bradshaw and F.M. Hoffmann. *Surf. Sci.* **72** (1978) 513.

[60] H. Ohtani, M.A. Van Hove, and G.A. Somorjai. *Surf. Sci.* **187** (1987) 372.

[61] H.A.C.M. Hendrickx, A.M.E. Winkelman, and B.E. Nieuwenhuys. *Appl. Surf. Sci.* **27** (1987) 458.

[62] W.F. Banholzer, Y.O. Park, K.M. Mak, and R.I. Masel. *Surf. Sci.* **128** (1985) 176.

[63] J.M. Gohndrone, Y.O. Park, and R.I. Masel. *J. Catalysis* **95** (1985) 244.

[64] E. Pelach, R.E. Viturro, and M. Folman. *Surf. Sci.* **161** (1985) 553.

[65] C. Klauber and B.G. Baker. *Appl. Surf. Sci.* **22/23** (1985) 486.

[66] S. Tatarenko, M. Alnot, and R. Ducros. *Surf. Sci.* **163** (1985) 249.

[67] L.H. Dubois, P.K. Hansma, and G.A. Somorjai. *J. Catalysis* **65** (1980) 318.

Table 1: Summary of structural parameters (in Å) that have been used in the dynamical LEED analysis of Rh(111)-(2x2)-3NO. The first and third numbers in each column represent the range of variation of the corresponding parameter, the step being shown between parentheses.

Model	$d_{\perp}$(Rh-NO)	$d_{\perp}$(N-N)	$d_{\parallel}$(N-N)	$d_{\perp}$(N-O)
1-bridge/2-top	1.25(0.1)1.65	0.1(0.1)0.8	2.2(0.1)3.0	1.05(0.1)1.35
1-top/2-bridge	1.5(0.1)1.9	0.2(0.1)0.6	2.6(0.1)3.4	1.05(0.1)1.35
1-top	1.5(0.1)1.9	—	—	0.95(0.1)1.35
1-bridge	1.25(0.1)1.65	—	—	0.95(0.1)1.35
1-hollow(both)	1.25(0.1)1.65	—	—	0.95(0.1)1.35

Table 2: Summary of best LEED R-factors (averaged over 5 R-factors) between theory and experiment for different models of Rh(111)-(2x2)-3NO.

Model	$d_{\perp}$(Rh-NO)	$d_{\perp}$(N-N)	$d_{\parallel}$(N-N)	$d_{\perp}$(N-O)	R-factor
1-bridge/2-top	1.55	0.5	2.6	1.15	0.279
1-top/2-bridge	1.70	0.2	2.8	1.15	0.298
1-top	1.70	—	—	1.15	0.358
1-bridge	1.55	—	—	1.05	0.359
1-hollow(both)	1.25	—	—	1.15	0.362

Table 3: Structural result in the format of the Surface Crystallographic Information Service (SCIS) handbook.[41]

SURFACE:

Substrate: Rh
Face: (111)
Bulk structure: fcc
Temperature: 30K
Adsorbate: NO
Surface pattern: (2x2), (2,0/0,2)
Adsorbate state: molecular
Coverage: 0.75(NO/Rh)

STRUCTURE:

Reference unit cell: a=5.36Å, b=5.36Å, A(a,b)=60°
2D symmetry: pm
Thermal vibrations: θ_D=406K(Rh), 920K(N), 861K(O)
R-factors: R_{VHT}=0.279, R_{ZJ}=0.260, R_{PE}=0.670

Layer	Atom	Atom positions		Normal layer spacing	Error
A1	O	0.2777	0.2777	0.0	-
A2	O	0.7223	0.7223	0.5	0.1
A3	O	0.0	0.0	0.65	-
A4	N	0.2777	0.2777	0.0	-
A5	N	0.7223	0.7223	0.5	0.1
A6	N	0.0	0.0	1.55	0.1
S1	Rh	0.25	0.25	0.0	-
S2	Rh	0.75	0.25	0.0	-
S3	Rh	0.25	0.75	0.0	-
S4	Rh	0.75	0.75	2.188	-
S5	Rh	0.0833	0.0833	0.0	-
S6	Rh	0.5833	0.0833	0.0	-
S7	Rh	0.0833	0.5833	0.0	-
S8	Rh	0.5833	0.5833	2.188	-

Table 4: Summary of bond lengths d and interlayer spacings $d_\perp$ (in Å), and of adsorption sites for NO or CO on Rh(111), as determined by LEED analysis.

Adsorbate(s)	d(Rh-NO) or d(Rh-CO)	$d_\perp$(Rh-NO) or $d_\perp$(Rh-CO)	d(N-O) or d(C-O)	NO or CO adsorption site
$(\sqrt{3}x\sqrt{3})R30°$-CO	1.95±0.1	1.95±0.1	1.07±0.1	top
(2x2)-3CO	1.94±0.1	1.87±0.1	1.15±0.1	near top
	2.03±0.1	1.52±0.1	1.15±0.1	bridge
c(4x2)-CCH_3+CO	2.02±0.03	1.30±0.05	1.18±0.05	hcp hollow
(2x2)-3NO	2.07±0.1	2.05±0.1	1.15±0.1	near top
	2.05±0.1	1.55±0.1	1.15±0.1	bridge
c(4x2)-CCH_3+NO	2.02±0.03	1.30±0.05	1.18±0.05	fcc hollow

Table 5: Assignments of peaks in HREEL spectra for NO on surfaces of various metals M.

Substrate	Adsorption Site	ν(N-O) (cm^{-1})	ν(M-NO) (cm^{-1})	δ(M-NO) (cm^{-1})	References
Ni(111)	bent	1490	400	740	[12]
	bridge	1600	375	—	
Pd(111)	bridge	1510-1660	460-490	—	[51]
	top	1720-1850	510-550	—	
Pd(100)	bridge	1505-1510	—	—	[55]
	top	1660-1720	—	—	
Pt(111)	bridge	1476-1516	306	—	[52, 53, 54]
	top	1700-1725	450	—	
Pt(100)-(1x1)	bent	1645	230	380	[14]
Pt(100)-(5x20)	bent	1690-1790	310	465	[14]
Rh(111)	bridge	1480-1635	405	—	[17],this work
	top	1815-1840	485	—	
Rh(111)+CCH_3	fcc hollow	1405-1435	—	—	[22]
Rh(100)	bent	910	—	—	[57]
	bridge	1600	—	—	
Rh(331)	bent	1704	—	403	[67]
	top	1815	—	—	
Ru(001)	hollow	1400	680	—	[48, 49, 50]
	bridge	1500	410	—	
	top	1783-1823	510-570	—	

Figure Captions

Figure 1: Specular HREEL spectra as a function of adsorption temperature and dosage. All spectra were recorded at 95 K. (A) 0.8 L NO dosed at 120 K. LEED showed a c(4x2) pattern. (B) 10 L NO dosed at 120 K. LEED showed a disordered pattern. (C) 25 L NO dosed after step (B) at 250 K; a new sharp (2x2) LEED pattern was observed.

Figure 2: Specular HREEL spectra as a function of annealing temperature. All spectra were taken at 95 K. (A) 25 L NO dosed at T = 250 K; this spectrum is similar to that in figure 1C. (B) Subsequent annealing to T = 360 K; LEED showed a disordered pattern. (C) T = 480 K, where complete dissociation of NO was observed; LEED showed a disordered pattern.

Figure 3: Side and top views of the best-fit model of the (2x2)-3NO structure, shown in top and bottom panels, respectively.

Figure 4: Experimental LEED intensity vs. voltage (I-V) curves for three different ordered structures: (2x2)-3NO (continuous lines), (2x2)-3CO [36, 37] (long-dash lines), and (2x1)-O [39] (short-dash lines), on the Rh(111) surface.

Figure 5: Comparative top view of Rh(111)-(2x2)-3NO and Rh(111)-(2x2)-3CO. Van der Waals radii of NO and CO molecules are used to indicate the close proximity between adsorbates within a (2x2) unit cell at 0.75 monolayer coverage. The radii for each atom are: N=1.55 Å, C=1.67 Å, O=1.50 Å.

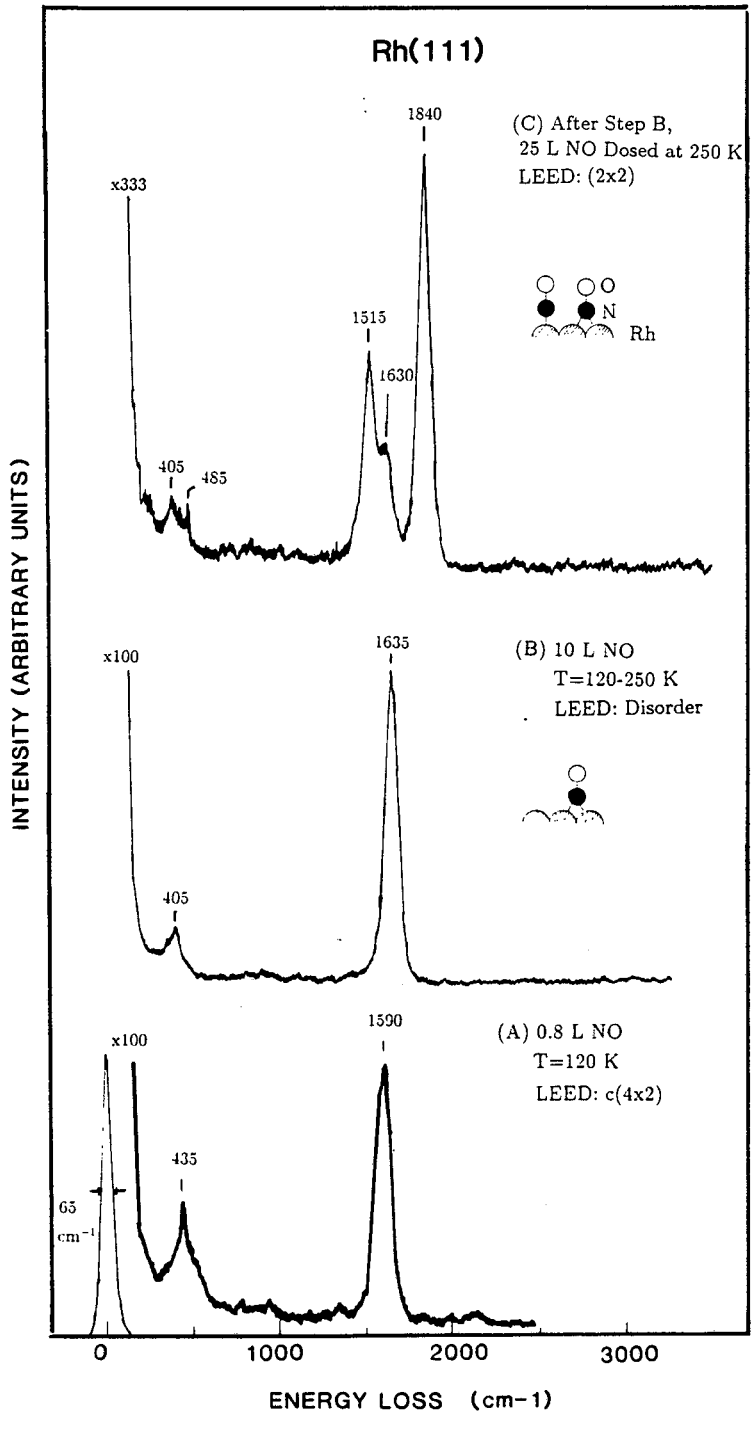

XBL 889-3252

Fig. 1

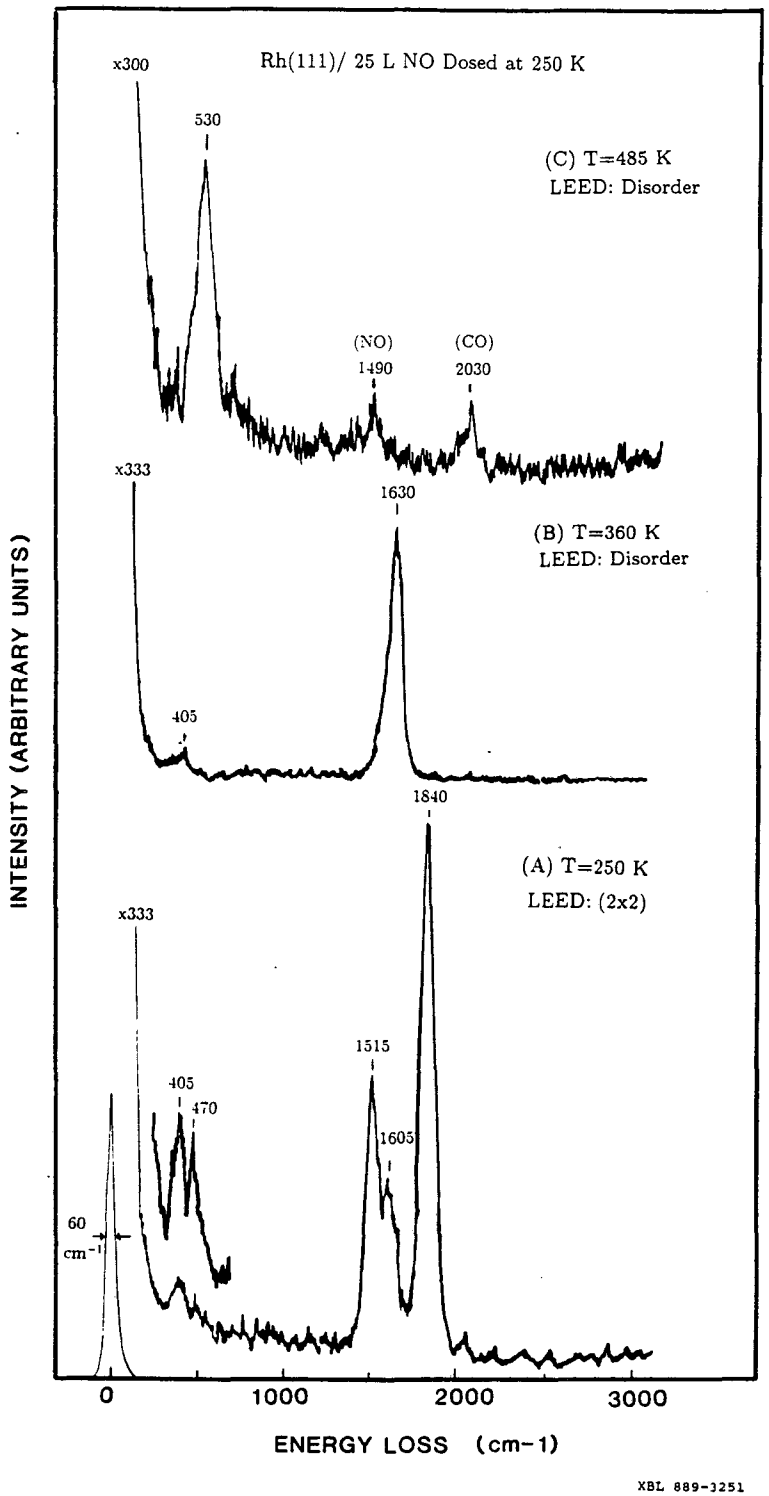
Rh(111)/ 25 L NO Dosed at 250 K
x300
530
(C) T=485 K
LEED: Disorder
(NO)
1490
(CO)
2030
x333
1630
(B) T=360 K
LEED: Disorder
405
1840
(A) T=250 K
LEED: (2x2)
x333
1515
405
470
1605
60
cm-1
INTENSITY (ARBITRARY UNITS)
0
1000
2000
3000
ENERGY LOSS (cm-1)
XBL 889-3251

Fig. 2

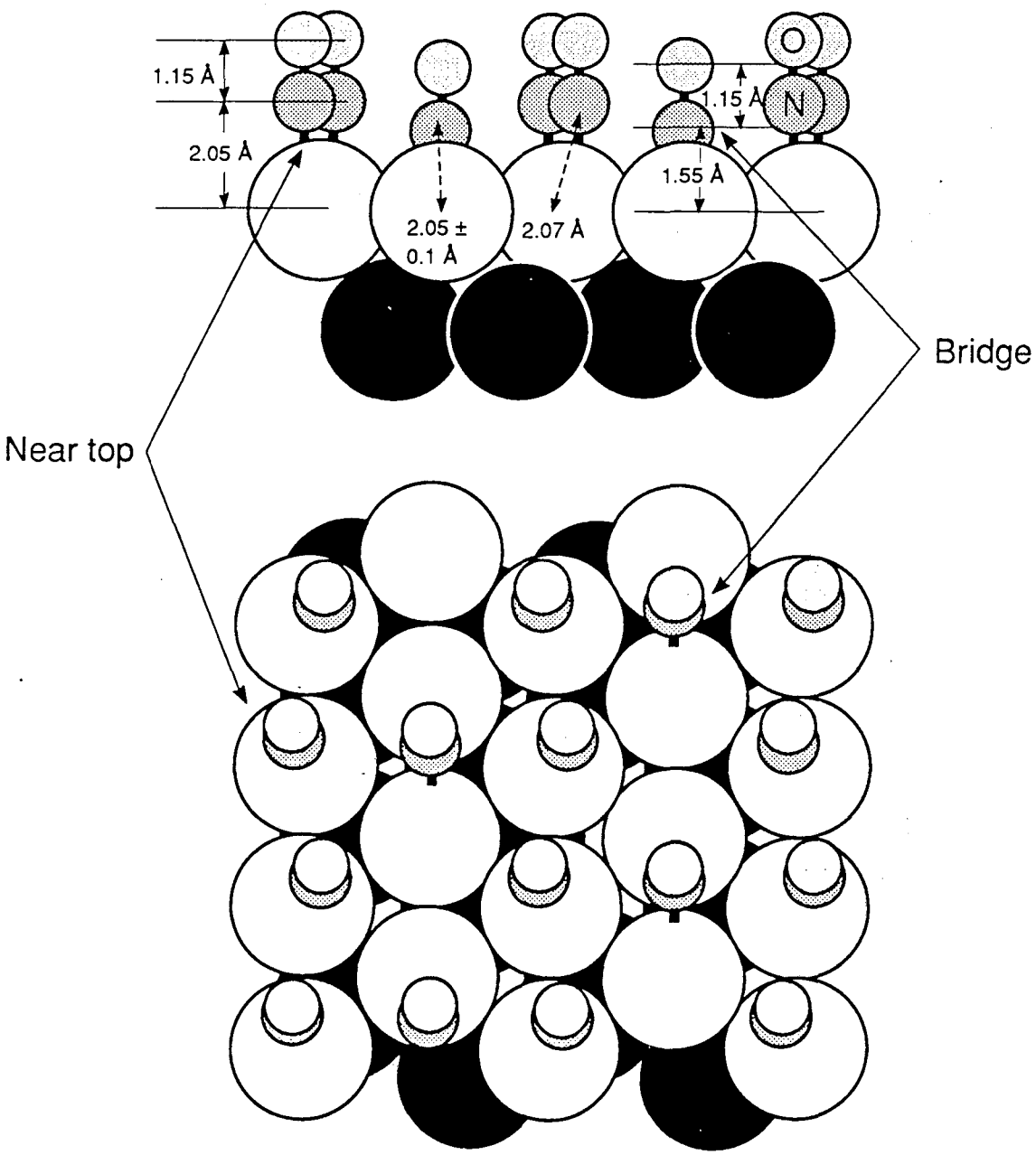

Rh(111) + (2 X 2) 3NO

XBL 888-8950

Fig. 3

I-V Curve Comparison

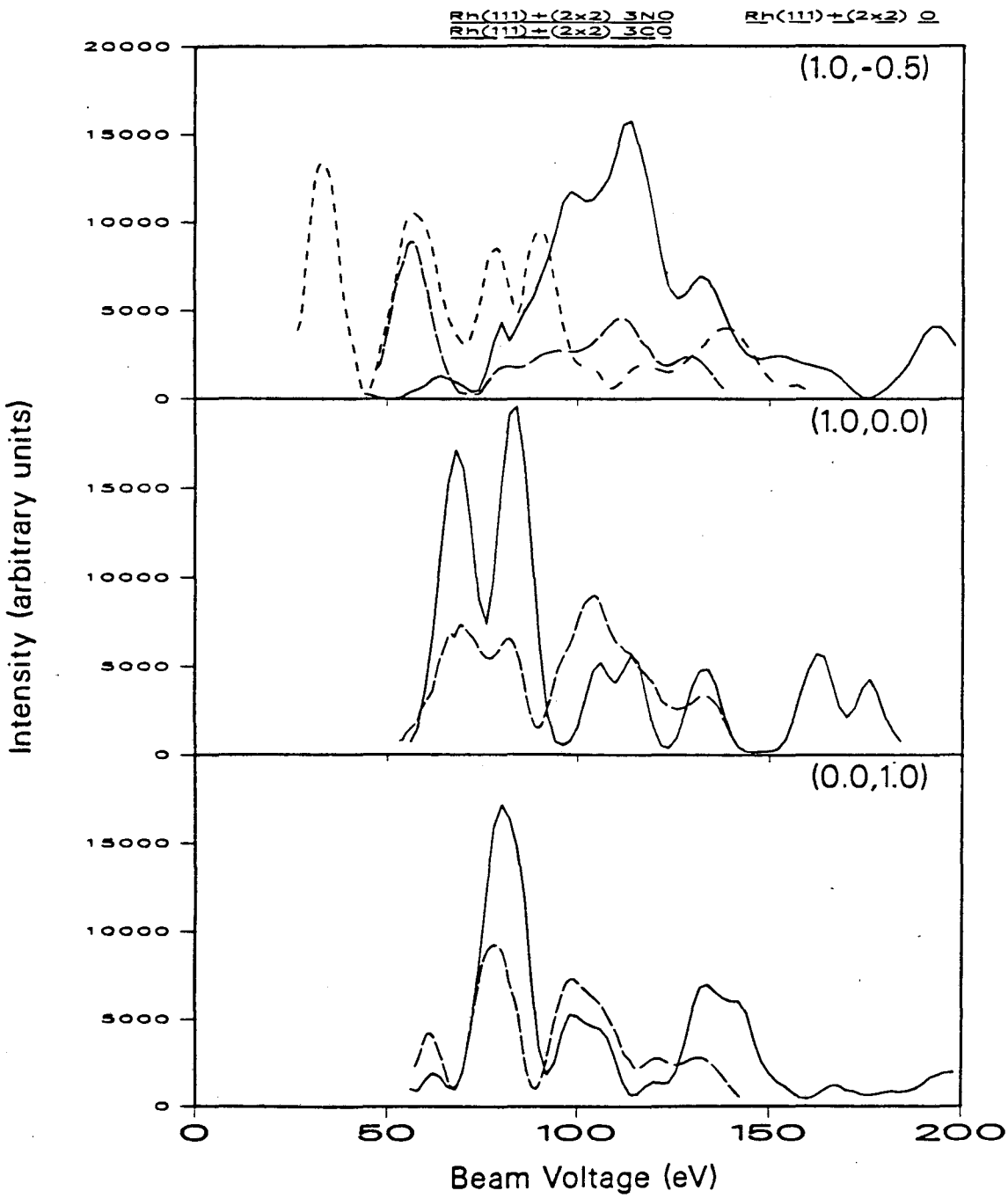

XBL 889-3238

Fig. 4

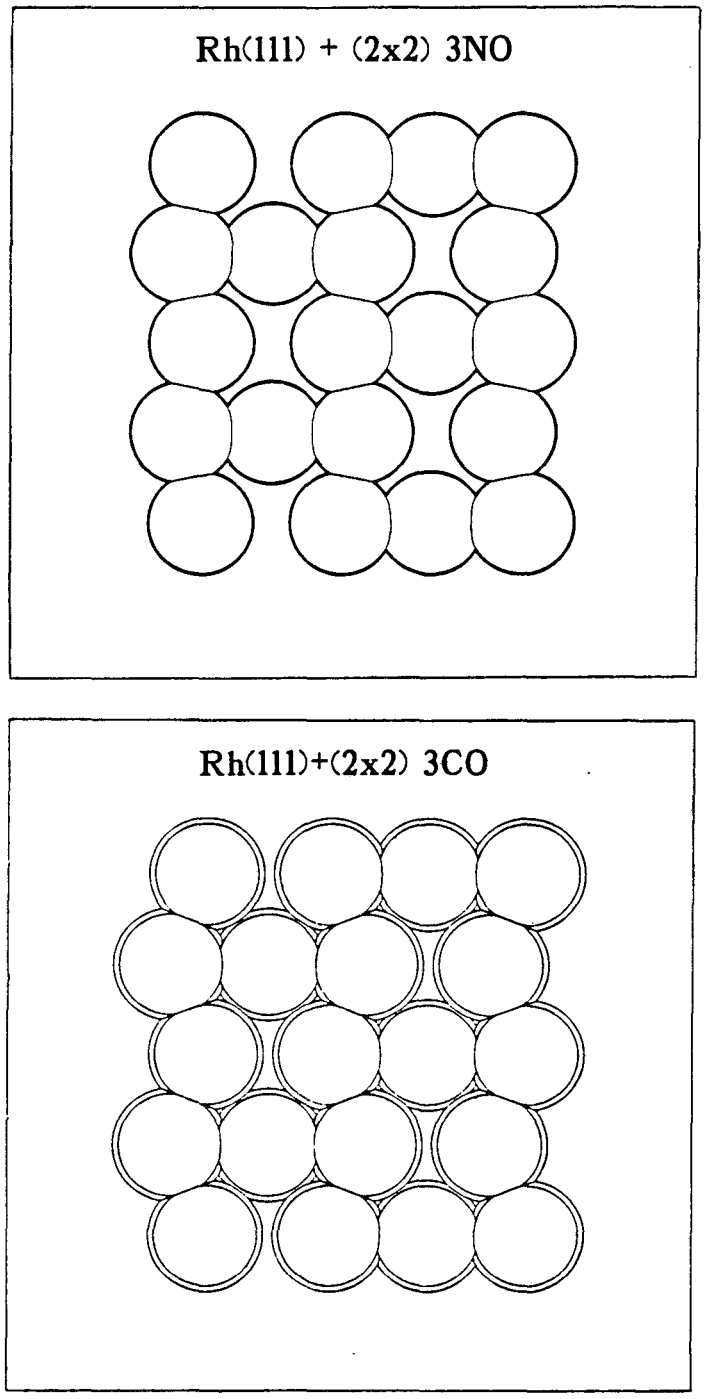

XBL 889-3249

Fig. 5

LAWRENCE BERKELEY LABORATORY
CENTER FOR ADVANCED MATERIALS
1 CYCLOTRON ROAD
BERKELEY, CALIFORNIA 94720